

Investigation of External Factors for Wireless Capacitive Power Transfer Systems

Mehmet Zahid EREL*, Kamil Cagatay BAYINDIR, Mehmet Timur AYDEMIR

Abstract: Capacitive power transfer (CPT) technology has gained more and more importance in recent years. This paper investigates the effects of temperature and relative humidity on CPT system performance. The conventional four-plate horizontal and vertical coupler structures are built to observe the variations of coupling capacitances under external factors. The pressure of the coupler ambient is kept constant, and the effects of temperature and relative humidity are reviewed separately. The different temperature (25 - 105 °C) and relative humidity (43 - 80% RH) levels are reviewed in these scenarios. The obtained results indicate that the values of coupling capacitances are inversely proportional to the temperature level, whereas the values of coupling capacitances are directly proportional to the relative humidity level. In addition, the visible changes happen in coupling capacitances after 45 °C and 55 °C for horizontally and vertically arranged four-plate coupler structures, respectively. It is also observed that relative humidity level becomes a critical point after 60% RH for both coupler structures. Among the coupling capacitances, the main capacitances are the most affected during the variations for both couplers. This study is expected to be a reference for the researchers on external factors in CPT systems.

Keywords: capacitive coupling; capacitive power transfer; relative humidity; temperature; wireless power transfer

1 INTRODUCTION

Wireless charging technology is becoming more preferred and widespread with a safe, reliable, and easy-to-use operation without plugs and wires. Among the wireless power transfer (WPT) technologies, inductive power transfer (IPT) and capacitive power transfer (CPT) are the most extensively utilized. While the IPT uses high-frequency magnetic fields [1], the CPT utilizes high-frequency electric fields to transfer power wirelessly [2].

The CPT technology has many advantages compared to IPT technology, such as lower cost, lightweight, better misalignment tolerance, and higher reliability [3]. Due to these advantages, it has many application areas varying from low power to high power levels. The prominent low-power applications can be stated as biomedical implants [4], and portable device charging [5]. Herein, the transfer distance is typically within the millimetre range, and the value of coupling capacitance is usually in the nanofarad range.

Considering high power applications, electric vehicle charging application becomes prominent [6]. The transfer distance has 100s of millimetre ranges, and the value of coupling capacitance is usually in the picofarad range. The circuit topology of a conventional CPT system is given in Fig. 1. The primary side is formed with an inverter and a compensation network, and the secondary side includes a compensation network and a rectifier.

The capacitive coupler, called coupling interface, requires metal plates along with the medium as a dielectric. The capacitive coupler has a significant role in power transfer from the primary side to the secondary side of the CPT system. The coupler structures are classified as the number of metal plates used and of positional characteristics. Among them, the four-plate coupler is generally used in CPT systems. Herein, two plates serve as a power transmitter, and the other two plates serve as a power receiver. In addition, the four-plate coupler structure is arranged horizontally and vertically in CPT applications. All in all, the capacitive coupler behaves as a resonant capacitance in the CPT system. Meanwhile, capacitance measurement plays a key role in high-frequency

applications as well. The value of coupling capacitance mainly depends on the dielectric material used, the distance between the metal plates, and the area of the metal plates. Hence, the dielectric material plays a key role in determining the main capacitance. The material properties of dielectrics are the relative permittivity (ϵ_r), electric field breakdown (kV/mm), and dielectric loss ($\tan\delta$). For instance, the relative permittivity of air is 1 at 20 °C, the electric field breakdown is 3 kV/mm, and the dielectric loss is 0. As silicon material, the relative permittivity is 11.8, the electric field breakdown is 30 kV/mm, and the dielectric loss is 5×10^{-3} at 1 GHz [7]. The relative permittivity of air depends on pressure (kpa), temperature (°C), and relative humidity (RH) [8]. For this reason, Rozario et al. mention factors that impact coupling capacitance in CPT systems [9]. Herein, the factors are described as voltage stress across the coupler, transfer distance, operational frequency, and atmospheric conditions. However, the external factors are not thoroughly reviewed in CPT systems. The external factors are examined in terms of temperature effects on the performance of the wireless IPT systems [10-14]. Mohsan et al. reviewed pressure, temperature, biofouling, and water conductivity factors for underwater wireless IPT applications [15]. The core, coil, and steel parts are negatively affected by increasing temperature. The increased pressure affects magnetizing inductance, the biofouling causes misalignments, and the increased seawater conductivity results in eddy currents. Hence, external factors influence wireless charging performance.

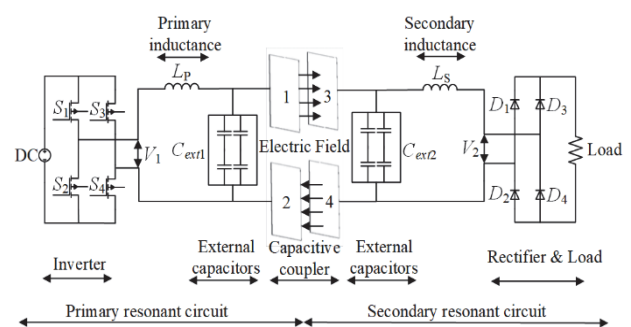


Figure 1 The circuit topology of a conventional CPT system

The role of dielectric materials is also reviewed in CPT systems, specifically using ceramic coatings [16], glass material [17], and air dielectric material [7]. The authors concluded that power transfer capability, increased coupling capacitance, and electric field breakdown strength are improved by utilizing various dielectric materials. Nevertheless, the external factors are not discussed due to the integration of dielectric materials. The effect of temperature is examined on the parasitic capacitance of the tapered through silicon [18]. The impact of relative humidity is investigated on surface mount solid tantalum capacitors [19]. Both relative humidity and temperature effects are reviewed in alumina coatings [20] and electrochemical sensors [21]. However, the dielectric constant of air is neither reviewed nor adopted to WPT systems.

Our paper differs from the other papers in that this paper focuses on both temperature and humidity effects on the behaviour of the CPT systems. For this reason, four plate horizontal and vertical coupler structures are designed for wireless CPT applications. As the relative humidity level of the coupler ambient keeps constant, different temperature levels are first implemented to the designed capacitive couplers. According to the obtained results, the capacitance of the coupler is inversely proportional to the increased temperature. Then, the relative humidity variations on capacitive coupler ambient are examined in this study. Thus, the capacitance of the coupler is directly proportional to the increased relative humidity level. The effect of temperature and relative humidity on the performance of the CPT system is verified by the integration of external factors. For this reason, a comparative study is presented in Tab. 1 to illustrate the differences and novelty of the proposed method for wireless charging applications.

The rest of the paper is organized as follows: Following the introductory section, four-plate capacitive coupler structures and their coupling capacitances are discussed in Section 2. Then, the experimental setup is described to validate the effectiveness of the proposed method for four-plate horizontal and vertical capacitive coupler structures. Moreover, the obtained results are discussed depending on the designed prototypes in Section 3. Finally, conclusions are drawn in Section 4.

Table 1 Comparison table for wireless charging applications under external factors

Reference	Wireless Technology	External Factors	Frequency
This work	Capacitive	Temperature and relative humidity effects for CPT systems	1 MHz
[10]	Inductive	Temperature effects for the efficiency of the IPT system	20 kHz
[13]	Inductive	Thermal analysis of dynamic wireless EV charging	85 kHz
[14]	Inductive	Thermal effects on wireless modules for EV charging	85 kHz
[12]	Inductive	Thermal design optimization for the IPT system	85 kHz

2 FOUR-PLATE CAPACITIVE COUPLER STRUCTURES

Capacitive coupler structures provide power transfer ability for CPT systems. The structure and dimensions of the four-plate horizontal and vertical capacitive coupler

structures are shown in Fig. 2. Fig. 2a represents four-plate horizontal structure [22], and Fig. 2b represents four-plate vertical structure [23]. As a horizontally arranged structure, P_1 and P_2 are used as power transmitters, and P_3 and P_4 are utilized as power receivers. The plate lengths of the coupler are defined as l_1 and l_2 . The distance between the same side plates is described as d_1 . The transfer distance is defined as d . The plate thickness is represented as t_p . Since the vertical coupler structure, P_1 and P_2 are the power transmitters, P_3 and P_4 are also the power receivers. The plates are designed to be square-shaped. As shown in Fig. 2b, P_1 and P_3 are larger than P_2 and P_4 . The lengths of the larger plates are l_3 , and the lengths of the smaller plates are l_4 . The transfer distance is defined as d_g , and the distance between the same side plates is d_c .

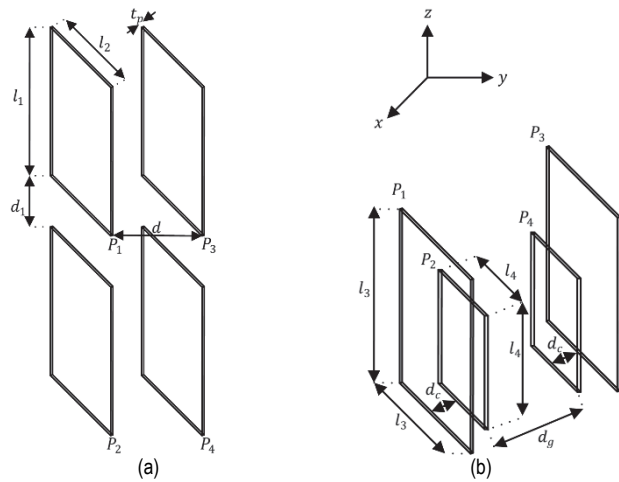


Figure 2 The four-plate coupler structures: (a) horizontal, (b) vertical

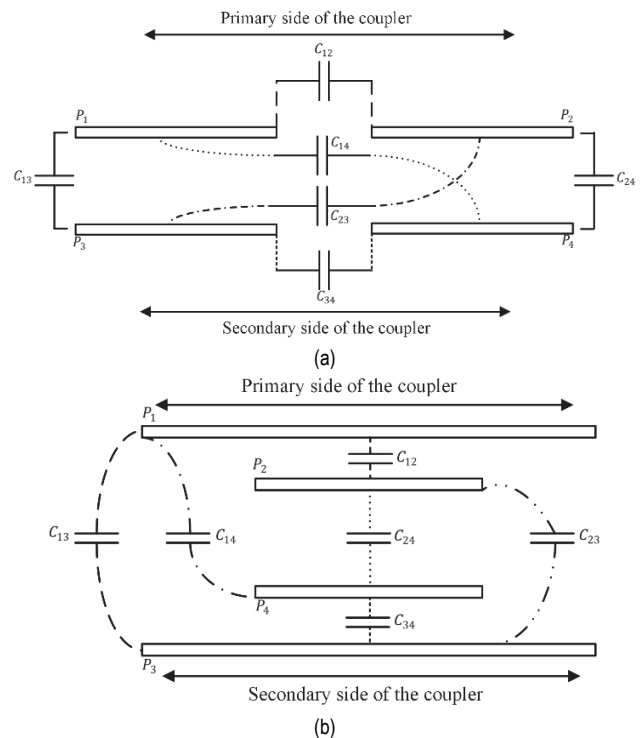


Figure 3 The four-plate coupler structures: (a) horizontal, (b) vertical

The coupling capacitors emerged based on the positioning of the metal plates and are represented in Fig. 3. Fig. 3a depicts the coupling capacitors in a four-plate

horizontal structure [22], and Fig. 3b represents the coupling capacitors in a four-plate vertical structure [23].

The four plates form six coupling capacitances. Herein, C_{12} and C_{34} are closely associated with the self-capacitances of the capacitive coupler. C_{14} and C_{23} are defined as cross-coupling capacitances. It is noteworthy that if there is a misalignment condition between the primary and secondary sides, cross-coupling capacitances should be considered. C_{13} and C_{24} are defined as main capacitances and thus play a key role in determining the resonant capacitance of the CPT system. The four-plate vertical structure has higher coupling capacitances and misalignment ability than the four-plate horizontal structure. While the four-plate horizontal structure is more prevalent in the literature due to its practical feature, the four-plate vertical structure is prominent, especially in recent studies such as rotary applications. The C_{12} and C_{34} are the main capacitances and are larger than C_{14} , C_{23} , C_{13} and C_{24} . Therefore, the main capacitances become prominent in a four-plate vertical structure to obtain the desired resonant capacitance.

Since four-plate horizontal and vertical capacitive coupler structures, the values of primary and secondary resonant capacitances and mutual capacitance are determined utilizing coupling capacitances given in Eq. (1) to Eq. (3) [24]. It is obvious that coupling capacitances considerably affect the CPT system performance.

$$C_p = C_{12} + \frac{(C_{13} + C_{14}) \cdot (C_{23} + C_{24})}{C_{13} + C_{14} + C_{23} + C_{24}} \quad (1)$$

$$C_s = C_{34} + \frac{(C_{13} + C_{23}) \cdot (C_{14} + C_{24})}{C_{13} + C_{14} + C_{23} + C_{24}} \quad (2)$$

$$C_M = \frac{(C_{24}C_{13}) - (C_{14}C_{23})}{C_{13} + C_{14} + C_{23} + C_{24}} \quad (3)$$

3 EXPERIMENTAL PROCEDURES

3.1 Experimental Design and Prototyping

Experimental prototypes are constructed in a four-plate capacitive coupler structure having horizontal and vertical arrangements. With the parameters in Tab. 2, the proposed system designs for horizontally and vertically arranged capacitive coupler structures are shown in Fig. 4 and Fig. 5, respectively. The small woods are used for both system designs to hold the metal plates and determine the desired transfer distance. Considering temperature measurement, the relative humidity level (RH %) is kept constant. BMK XH-W3001 digital thermostat as a temperature controller is used to set the temperature level and TM902C digital thermometer ($-50, 750 \text{ }^\circ\text{C}$) is utilized to observe the temperature variations. To determine the effects of relative humidity variations on the capacitive coupler environment, a W-712B mist generator is utilized along with an HTC-1 relative humidity meter. The operating frequency is set to 1 MHz for temperature and relative humidity measurements using GW Instek LCR-8101G meter.

Considering proposed designs, the system working principle depends on the coupling capacitance variations

when the temperature and relative humidity level of the coupler change separately. First, the relative humidity (RH %) level is kept constant for both designs and, the temperature level is set from 25 to 105 $^\circ\text{C}$ with an increment of 10 $^\circ\text{C}$. The two pieces of bulbs are used for heating to gradually increase the temperature in a closed environment. Hence, the temperature increment is achieved in desired ranges. The nine different temperature levels are recorded, and the values of coupling capacitances are observed.

Second, the effect of relative humidity on capacitive coupler structures is evaluated by keeping the temperature level constant. The relative humidity level is set from 43 to 80 (RH %) with an increment of about 10%. The mist generator is utilized to obtain the desired relative humidity levels in a closed environment. The five different relative humidity levels are recorded, and the changes of the coupling capacitances are reviewed.

Table 2 System specifications and parameter values

Parameter	Definition	Value
l_1	The length of horizontally arranged plates in the z -direction.	180 mm
l_2	The length of horizontally arranged plates in the y -direction.	75 mm
l_3	The length of larger plates in vertically arranged coupler.	100 mm
l_4	The length of smaller plates in vertically arranged coupler.	50 mm
d	Air-gap for horizontally arranged coupler.	150 mm
d_1	Distance between the same side plates for horizontally arranged coupler.	40 mm
d_c	Distance between the same side plates for vertically arranged coupler.	2 mm
d_g	Air-gap for vertically arranged coupler.	5 mm
t_p	Plate thickness.	2 mm



Figure 4 The designed system using four-plate horizontal capacitive coupler structure: (1) LCR meter, (2) digital thermometer, (3) horizontal coupler, (4) bulb, (5) humidity meter, (6) temperature controller

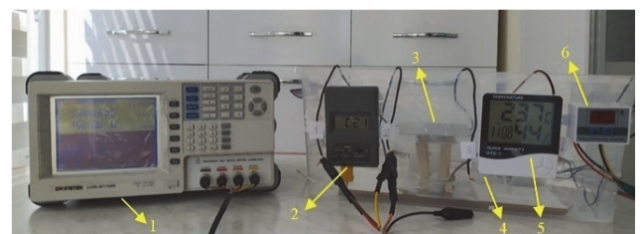


Figure 5 The designed system using four-plate vertical capacitive coupler structure: (1) LCR meter, (2) digital thermometer, (3) vertical coupler, (4) bulb, (5) humidity meter, (6) temperature controller

3.2 Experimental Results and Discussion

The effects of temperature and relative humidity are investigated based on the designed CPT systems which are presented in Fig. 4 and Fig. 5, respectively. Here we first reviewed four-plate horizontal structure as the relative

humidity level of the coupler environment keeps constant. Meanwhile, the pressure effect of the system also keeps constant. Then, four-plate vertical coupler structure is utilized to observe the behaviour of the CPT system under external factors. The parallel plate capacitor structure is used to build the four-plate coupler structures. Furthermore, the aluminium metal plates are also used to form the coupler structures. The dielectric constant of air is inversely proportional to the temperature rising and directly proportional to the relative humidity rising [25]. As a theoretical prediction of the experiments, the value of coupling capacitances should be proportional to the dielectric constant of air.

According to the horizontally arranged coupler structure, the changes in coupling capacitances based on the temperature variations are given in Tab. 3. There are significant variations in coupling capacitances, specifically main capacitances after 45 °C temperature level, as depicted in Fig. 6. The obtained results indicate that the coupling capacitances gradually decrease with the temperature increase.

The relative humidity effect on four-plate horizontally arranged CPT system is then evaluated in detail. The changes in coupling capacitances are given in Tab. 4. Herein, the biggest changes occur at main capacitances, C_{13} and C_{24} , as shown in Fig. 7, especially after the 60 % RH level. The obtained results show that the values of coupling capacitances rise along with increased relative humidity levels.

Afterwards, the temperature effect on the vertically arranged capacitive coupler structure is examined in detail. The changes in coupling capacitances based on the temperature variations are given in Tab. 5. There are crucial variations in coupling capacitances, specifically main capacitances after 55 °C temperature level, as depicted in Fig. 8. The obtained results indicate that the coupling capacitances gradually decrease with the temperature increase.

The relative humidity effect on four-plate vertically arranged CPT system is evaluated in detail. The changes in coupling capacitances are given in Tab. 6. Herein, the biggest changes occur at main capacitances, C_{12} and C_{34} , as shown in Fig. 9, especially after the 60% RH level. The obtained results show that the values of coupling capacitances rise concerning relative humidity level.

As a result, the values of coupling capacitances are inversely proportional to the temperature rise, while the relative humidity level is directly proportional. The values of main capacitances are more influenced by temperature and relative humidity variations for both designed systems. Considering the four-plate horizontal structure, the values of C_{13} and C_{24} decrease about 10 pF during temperature variation and increase roughly 8 pF during relative humidity variations. Considering the four-plate vertical structure, the values of C_{12} and C_{34} decrease by about 8 pF during temperature variations and increase by about 10 pF during relative humidity variations.

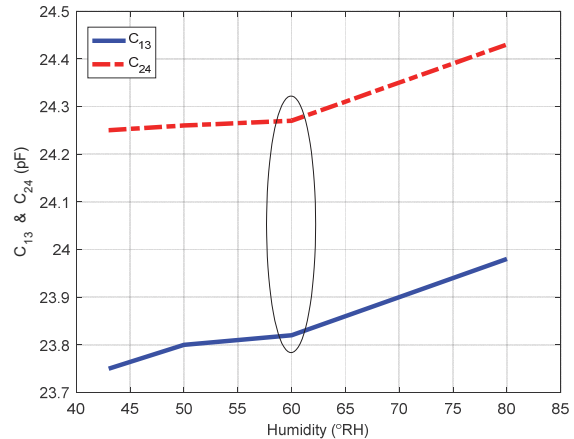


Figure 7 The changes in coupling capacitances based on the relative humidity variations in a four-plate horizontal structure

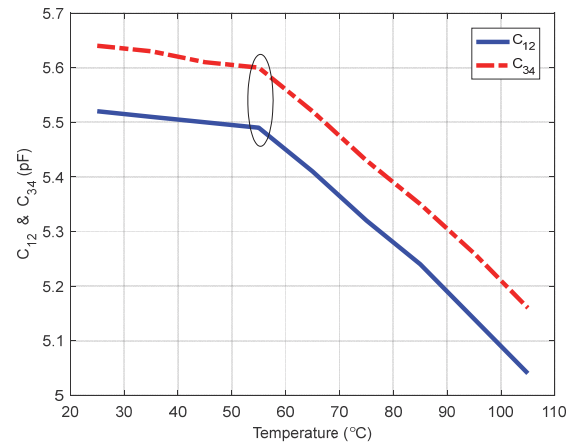


Figure 8 The changes in coupling capacitances based on the temperature variations in a four-plate vertical structure

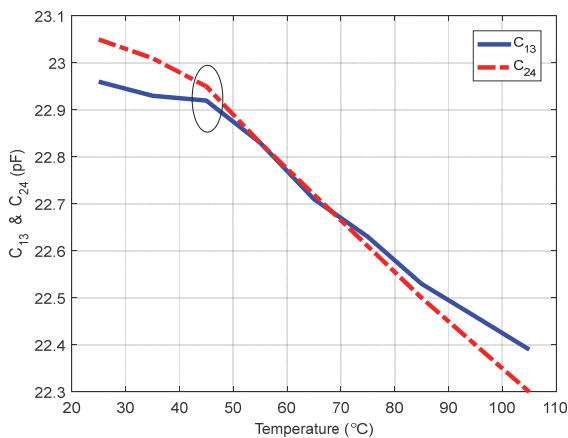


Figure 6 The changes in coupling capacitances based on the temperature variations in a four-plate horizontal

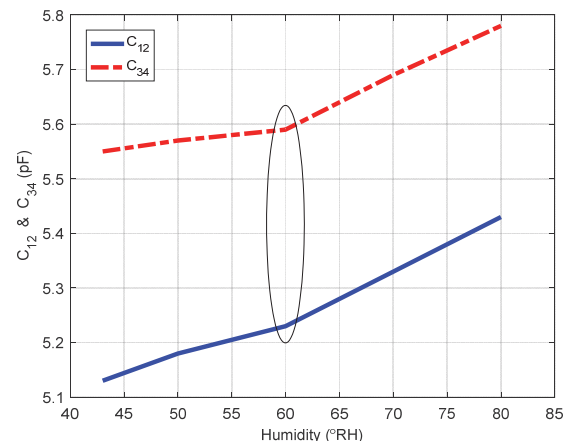


Figure 9 The changes in coupling capacitances based on the relative humidity variations in a four-plate vertical structure

Table 3 The values of coupling capacitances during temperature variations in a four-plate horizontal structure

Coupling capacitances / pF	Temperature levels								
	25 °C	35 °C	45 °C	55 °C	65 °C	75 °C	85 °C	95 °C	105 °C
C_{12}	2,58	2,57	2,56	2,52	2,48	2,43	2,39	2,35	2,30
C_{13} (main)	22,96	22,93	22,92	22,83	22,71	22,63	22,53	22,46	22,39
C_{14}	2,83	2,82	2,81	2,77	2,73	2,69	2,65	2,60	2,55
C_{23}	2,72	2,71	2,70	2,65	2,61	2,57	2,52	2,47	2,41
C_{24} (main)	23,05	23,01	22,95	22,83	22,72	22,61	22,50	22,40	22,30
C_{34}	3,11	3,10	3,09	3,04	3,00	2,95	2,90	2,86	2,81

Table 4 The values of coupling capacitances during relative humidity variations in a four-plate horizontal structure

Coupling capacitances / pF	Relative humidity levels				
	43% RH	50% RH	60% RH	70% RH	80% RH
C_{12}	3,46	3,51	3,55	3,59	3,63
C_{13} (main)	23,75	23,80	23,82	23,90	23,98
C_{14}	4,06	4,10	4,14	4,18	4,23
C_{23}	4,02	4,06	4,12	4,16	4,21
C_{24} (main)	24,25	24,26	24,27	24,35	24,43
C_{34}	5,23	5,27	5,31	5,35	5,39

Table 5 The values of coupling capacitances during temperature variations in a four-plate vertical structure

Coupling capacitances / pF	Temperature levels								
	25 °C	35 °C	45 °C	55 °C	65 °C	75 °C	85 °C	95 °C	105 °C
C_{12}	5,52	5,51	5,50	5,49	5,41	5,32	5,24	5,14	5,04
C_{13} (main)	4,40	4,39	4,37	4,36	4,33	4,29	4,25	4,20	4,15
C_{14}	2,95	2,94	2,92	2,91	2,87	2,83	2,77	2,73	2,68
C_{23}	3,39	3,38	3,36	3,35	3,33	3,30	3,26	3,22	3,17
C_{24} (main)	2,73	2,72	2,70	2,69	2,65	2,61	2,57	2,53	2,48
C_{34}	5,64	5,63	5,61	5,60	5,52	5,43	5,35	5,26	5,16

Table 6 The values of coupling capacitances during relative humidity variations in a four-plate vertical structure

Coupling capacitances / pF	Relative humidity levels				
	43% RH	50% RH	60% RH	70% RH	80% RH
C_{12}	5,13	5,18	5,23	5,33	5,43
C_{13} (main)	4,10	4,16	4,21	4,25	4,30
C_{14}	2,84	2,85	2,89	2,95	3,00
C_{23}	3,03	3,09	3,12	3,16	3,20
C_{24} (main)	2,52	2,55	2,56	2,60	2,64
C_{34}	5,55	5,57	5,59	5,69	5,78

4 CONCLUSION

This paper discusses temperature and relative humidity effects on capacitive coupler structures for wireless capacitive charging systems. Herein we introduce a CPT system with four-plate horizontal and vertical coupler structures to show the effects of external factors. The changes in coupling capacitances are considered to evaluate the behavioural characteristics of the CPT system during temperature and relative humidity variations using air as a medium. First, the temperature effect is investigated in both coupler structures keeping the relative humidity level constant. The temperature levels are set from 25 to 105 °C and adjusted with an increment of 10 °C using a temperature controller. According to the results, the temperature rising is inversely proportional to the values of coupling capacitances for both coupler structures. The visible changes in coupling capacitances happen after the temperature levels of 45 °C and 55 °C for horizontally and vertically arranged capacitive coupler structures, respectively. Nevertheless, remarkable changes occur in the main capacitances in comparison with the other

coupling capacitances. Conversely, the relative humidity effect is evaluated in four-plate capacitive coupler structures, maintaining a constant temperature for the coupler environment. For this reason, the relative humidity levels are considered within 43 - 80% RH levels. The obtained results indicate that relative humidity variations are directly proportional to the values of coupling capacitances. The visible changes in coupling capacitances happen after the relative humidity level of 60% for four-plate coupler structures. However, significant changes occur in the main capacitances compared to other coupling capacitances. In a nutshell, the temperature and relative humidity factors have significant influence on the resonances in the circuit. The results show that external factors change the values of coupling capacitances according to the capacitive coupler structure and play a critical role in resonance mechanism. They should be considered when designing the resonant circuitry, not only with CPT technology but also with IPT technology, especially for drone and underwater wireless charging applications that are significantly affected by temperature, humidity, and pressure factors. Future research will focus

on the pressure effect on capacitive coupler structures to validate the significance of external factors.

5 REFERENCES

- [1] Nataraj, C., Khan, S., Habaebi, M. H., & Muthalif, A. G. (2018). General analysis of resonance coupled wireless power transfer (Wpt) using inductive coils. *Tehnički vjesnik*, 25(3), 720-726. <https://doi.org/10.17559/TV-20160105041434>
- [2] Wang, Y., Zhang, H., & Lu, F. (2022). 3.5-kW 94.2% DC-DC Efficiency Capacitive Power Transfer With Zero Reactive Power Circulating. *IEEE Transactions on Power Electronics*, 38(2), 1479-1484. <https://doi.org/10.1109/tpel.2022.3215283>
- [3] Xia, J., Yuan, X., Lu, S., Li, J., Luo, S., & Li, S. (2021). A two-stage parameter optimization method for capacitive power transfer systems. *IEEE Transactions on Power Electronics*, 37(1), 1102-1117. <https://doi.org/10.1109/tpel.2021.3097344>
- [4] Tamura, M., Segawa, T., & Matsumoto, M. (2022). Capacitive Coupler for Wireless Power Transfer to Intravascular Implant Devices. *IEEE Microwave and Wireless Components Letters*, 32(6), 672-675. <https://doi.org/10.1109/lmwc.2022.3160688>
- [5] Zhu, J. Q., Ban, Y. L., Xu, R. M., & Mi, C. C. (2020). An NFC-CPT-combined coupler with series- π compensation for metal-cover smartphone applications. *IEEE Journal of Emerging and Selected Topics in Power Electronics*, 9(3), 3758-3769. <https://doi.org/10.1109/jestpe.2020.3002858>
- [6] Sinha, S., Kumar, A., Regensburger, B., & Afridi, K. K. (2019). A new design approach to mitigating the effect of parasitics in capacitive wireless power transfer systems for electric vehicle charging. *IEEE Transactions on Transportation Electrification*, 5(4), 1040-1059. <https://doi.org/10.1109/tte.2019.2931869>
- [7] Vincent, D. & Williamson, S. S. (2020, February). Role of dielectrics in the capacitive wireless power transfer system. *2020 IEEE International Conference on Industrial Technology (ICIT)*, 1217-1222. <https://doi.org/10.1109/icit45562.2020.9067136>
- [8] Zhang, B., He, J., & Ji, Y. (2019). Prediction of average mobility of ions from corona discharge in air with respect to pressure, humidity and temperature. *IEEE Transactions on Dielectrics and Electrical Insulation*, 26(5), 1403-1410. <https://doi.org/10.1109/TDEI.2019.008001>
- [9] Rozario, D., Azeez, N. A., & Williamson, S. S. (2016, June). Analysis and design of coupling capacitors for contactless capacitive power transfer systems. *2016 IEEE Transportation Electrification Conference and Expo (ITEC)*, 1-7. <https://doi.org/10.1109/itec.2016.7520244>
- [10] Hwang, K., Chung, S., Yoon, U., Lee, M., & Ahn, S. (2013). Thermal analysis for temperature robust wireless power transfer systems. *2013 IEEE Wireless Power Transfer (WPT)*, 52-55. <https://doi.org/10.1109/wpt.2013.6556879>
- [11] Mohammad, M., Onar, O. C., Pries, J. L., Galigekere, V. P., Su, G. J., & Wilkins, J. (2021). Thermal analysis of a 50 kW three-phase wireless charging system. *2021 IEEE Transportation Electrification Conference & Expo (ITEC)*, 1-6. <https://doi.org/10.1109/itec51675.2021.9490053>
- [12] Mohammad, M., Onar, O. C., Galigekere, V. P., Su, G. J., & Wilkins, J. (2022). Thermal Design and Optimization of High-Power Wireless Charging System. *2022 IEEE Applied Power Electronics Conference and Exposition (APEC)*, 480-485. <https://doi.org/10.1109/apec43599.2022.9773484>
- [13] Wojda, R., Galigekere, V. P., Pries, J., & Onar, O. (2020, June). Thermal analysis of wireless power transfer coils for dynamic wireless electric vehicle charging. *2020 IEEE Transportation Electrification Conference & Expo (ITEC)*, 835-838. <https://doi.org/10.1109/itec48692.2020.9161453>
- [14] Zimmer, S., Helwig, M., Lucas, P., Winkler, A., & Modler, N. (2020). Investigation of thermal effects in different lightweight constructions for vehicular wireless power transfer modules. *World Electric Vehicle Journal*, 11(4), 67. <https://doi.org/10.3390/wevj11040067>
- [15] Mohsan, S. A. H., Khan, M. A., Mazinani, A., Alsharif, M. H., & Cho, H. S. (2022). Enabling Underwater Wireless Power Transfer towards Sixth Generation (6G) Wireless Networks: Opportunities, Recent Advances, and Technical Challenges. *Journal of Marine Science and Engineering*, 10(9), 1282. <https://doi.org/10.3390/jmse10091282>
- [16] Ge, B., Ludois, D. C., & Perez, R. (2014). The use of dielectric coatings in capacitive power transfer systems. *2014 IEEE Energy Conversion Congress and Exposition (ECCE)*, 2193-2199. <https://doi.org/10.1109/ecce.2014.6953695>
- [17] Yi, K. H. (2016). High frequency capacitive coupling wireless power transfer using glass dielectric layers. *2016 IEEE Wireless Power Transfer Conference (WPTC)*, 1-3. <https://doi.org/10.1109/wpt.2016.7498857>
- [18] Liu, Y., Zhu, Z., Liu, X., Gu, H., & Guo, L. (2018). Temperature-dependent characterizations on parasitic capacitance of tapered through silicon via (T-TSV). *IEICE Electronics Express*, 15(24), 20180878-20180878. <https://doi.org/10.1587/elex.15.20180878>
- [19] Virkki, J. & Raunonen, P. (2011). Testing the effects of sea coast atmosphere on tantalum capacitors. *Active and Passive Electronic Components*, 2011. <https://doi.org/10.1155/2011/108423>
- [20] Niittymäki, M., Lahti, K., Suhonen, T., & Metsäjoki, J. (2018). Effect of temperature and humidity on dielectric properties of thermally sprayed alumina coatings. *IEEE Transactions on Dielectrics and Electrical Insulation*, 25(3), 908-918. <https://doi.org/10.1109/tdei.2018.006892>
- [21] Chani, M. T. S., Karimov, K. S., Bakhsh, E. M., & Rahman, M. M. (2022). Effect of Humidity and Temperature on the Impedances and Voltage of Al/Gr-Jelly/Cu-Rubber Composite-Based Flexible Electrochemical Sensors. *Gels*, 8(2), 73. <https://doi.org/10.3390/gels8020073>
- [22] Lu, F., Zhang, H., Hofmann, H., & Mi, C. C. (2017). A double-sided LC-compensation circuit for loosely coupled capacitive power transfer. *IEEE transactions on power electronics*, 33(2), 1633-1643. <https://doi.org/10.1109/tpel.2017.2674688>
- [23] Zhang, H., Lu, F., Hofmann, H., Liu, W., & Mi, C. C. (2016). A four-plate compact capacitive coupler design and LCL-compensated topology for capacitive power transfer in electric vehicle charging application. *IEEE Transactions on Power Electronics*, 31(12), 8541-8551. <https://doi.org/10.1109/tpel.2016.2520963>
- [24] Mi, C. (2015). High power capacitive power transfer for electric vehicle charging applications. *2015 6th international conference on Power Electronics Systems and Applications (PESA)*, 1-4. <https://doi.org/doi:10.1109/pesa.2015.7398937>
- [25] Choi, J. M. & Kim, T. W. (2013). Humidity sensor using an air capacitor. *Transactions on Electrical and Electronic Materials*, 14(4), 182-186. <https://doi.org/10.4313/teem.2013.14.4.182>

Contact information:

Mehmet Zahid EREL, PhD
(Corresponding author)
Department of Energy Systems Engineering,
Ankara Yildirim Beyazit University
Ankara, 06010, Turkey
E-mail: mzerel@ybu.edu.tr

Kamil Cagatay BAYINDIR, PhD, Full Professor
Department of Electrical and Electronics Engineering,
Ankara Yildirim Beyazit University,
Ankara, 06010, Turkey
E-mail: kcbayindir@ybu.edu.tr

Mehmet Timur AYDEMİR, PhD, Full Professor
Department of Electrical and Electronics Engineering,
Kadir Has University,
Istanbul, 34083, Turkey
E-mail: timur.aydemir@khas.edu.tr